Fundamental thermodynamic properties of sorbents for atmospheric water capture

*Authors: Ulrich Legrand [a], Juan Ricardo Castillo Sánchez [b], Richard Boudreault [c], Jean-Luc Meunier [d], Pierre-Luc Girard Lauriault [d], Jason Robert Tavares [a]**

Affiliations:

[a] CREPEC, Chemical Engineering Department, Polytechnique Montreal, 2500 Chemin de Polytechnique, Montréal, Qc, H3T 1J4, Canada

[b] Centre for Research in Computational Thermochemistry (CRCT), Department of Chemical Engineering, Polytechnique Montréal, University of Montreal Campus, 2500 Chemin de Polytechnique, Montreal, Qc, H3T 1J4 Canada

[c] Awn Nanotech, Inc., 1985 55th Ave, Suite 100, Dorval, Qc, H9P 1G9, Canada

[d] Department of Chemical Engineering, McGill University, 3610 University, Montréal, QC H3A 0C5, Canada

**corresponding author email: jason-robert.tavares@polymtl.ca*

Abstract: Thermodynamic properties of various sorbents, namely carbon-based sorbents, silica gel and metal-organic frameworks (MOFs) were assessed and compared based on their adsorption isotherms at 25, 30 and 35 °C. The isotherms were measured in a custom-made and calibrated environmental chamber using a gravimetric method. Gibbs free energy demonstrated the spontaneity of the adsorption process and the hygroscopicity variation of the sorbents depending on their surface chemistry. The carbon-based sorbent, nanoporous sponges (NPS), and one of the MOFs, Cr-MIL-101, had lower sorbent-adsorbate interactions and thus had integral enthalpies converging rapidly to the heat of vaporization of pure water. As such, these samples would release less heat during an adsorption step with partial filling of the sorbent. Integral entropy showed that, for most of the environmental conditions, adsorbed water molecules had an entropy equivalent to pure water for most of the sorbent materials, except for the silica gel due to its higher energy sites and higher water-sorbent interactions. NPS and Cr-MIL-101 were shown to be entropically

advantageous for the recovery/removal of water. Enthalpy and entropy can provide favorable conditions to perform adsorption-desorption cycles in a practical water capture system.

Keywords: sorbents, water adsorption, Gibbs free energy, enthalpy of adsorption, entropy

Graphical abstract:

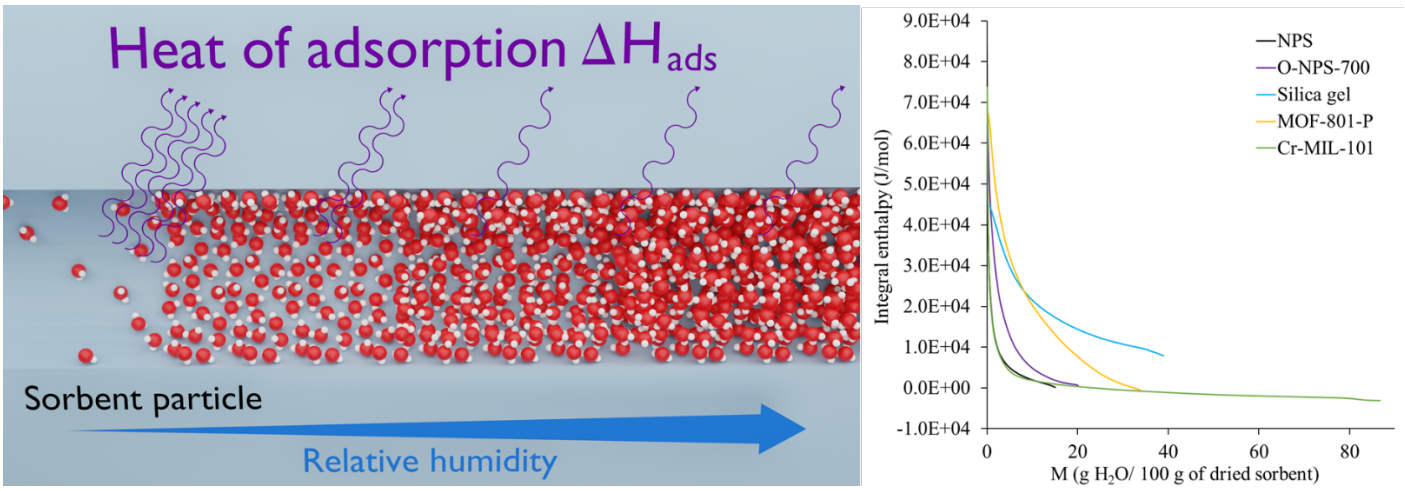

1. Introduction

Water is essential to all living beings. Across the globe, it is unevenly distributed with countries such as Canada having 20% of the total freshwater for 0.5% of the world's population [1] while the entire African continent has 9% of the freshwater resources for 16% of the world's population [2]. Freshwater access inequalities and sanitation issues meant that, in 2017, 55% of the world population lacked access to properly sanitized or sanitary water [3]. Climate change is likely to heighten the global water crisis. Indeed, rising temperatures will make some places drier, while places that are not currently threatened by water scarcity could see their situation change in the next decades [4]. Extreme weather events can also have a negative impact on the water supply, namely where floods and droughts could threaten the surface and groundwater quality and supply [5]. The atmosphere will become a larger water reservoir with rising temperatures. Water is currently supplied from available freshwater either from groundwater or from the surface, in lakes and rivers, or by desalination. Desalination is currently estimated to produce 95 million m3/day through nearly 15,900 operational plants, with half of this water produced in the Middle East and North Africa [6]. However, these plants also release massive volumes of brine, a high concentration saltwater solution with high disposal costs and detrimental to the environment [7]. Desalination is largely limited to coastal regions, while dry inland regions face the additional cost of transportation.

As such, innovation in water supply is required and might reduce the inequalities between the different world regions while helping countries better adapt to climate change. One of the most promising technologies, in this regard, is atmospheric water generation through water adsorption: a sorbent material is employed to spontaneously adsorb water and release it when provided with energy. The sorbents must be highly microporous, preferentially with narrow pore size

distributions minimizing hysteresis between adsorption and desorption [8]. Pore size is also important, it ensures that capillary condensation will occur: the critical pore size below which this mechanism will occur depends on the nature of the adsorbate and temperature. For example, argon at 77K has a critical pore size of 3.0 nm [9] while water at 298 K has a critical pore size of 2.2 nm [10]. Depending on the sorbent's surface chemistry, water will adsorb differently onto the active surface area. For hydrophilic surfaces, adsorbed water first arranges in molecule monolayers at low relative humidity. As relative humidity increases, water forms multilayers until menisci appear: this is capillary condensation [11], [12]. At higher relative humidity, the menisci grow and fill the micropores, and then after the mesopores. Do *et al.* described a theoretical model to explain the adsorption mechanism in hydrophobic porous material, and more specifically carbon-based sorbents [13]–[15]. They demonstrated that water adsorbs preferentially at functional groups dispersed on the carbon surface (i.e. primary adsorption site). These first water molecules then become secondary adsorption sites and water nuclei grow with increasing relative humidity. At some point, small water clusters of more than 5 molecules detach and subsequently fill the micropores and mesopores.

An optimal sorbent must present a set of attributes to reach commercial application: high water uptake, fast kinetics, low energy requirements, stability over adsorption-desorption cycles, capital and operational cost effectiveness and synthesis scalability. Several sorbents have been extensively studied in the literature for atmospheric water capture. Metal-organic frameworks (MOFs) are networks of metallic sites bonded with organic ligands in a crystalline structure whose porosity is tightly controlled. Some MOFs have been reported to reach water uptakes of more than 1 $kg_{water}/kg_{sorbent}$ (abbreviated as kg/kg) [16], and several promising MOF candidates were tested under real conditions [17]. However, MOFs sometimes suffer from poor hydrolytic stability, i.e.

the degradation of their structure in presence of water [18], and require complex synthesis processes that limit scalability. Efforts in the field of MOFs scale-up have identified avenues to facilitate synthesis with the help of microwaves or electrochemistry [19]. On the other hand, silica gel has a known commercial availability, and is one of the most studied sorbents for dehumidification purposes. For atmospheric water capture, silica gel has drawbacks, and notably has a strong interaction with water molecules due to its high surface concentration of hydroxyl groups, making the desorption step energy intensive [20]. This is namely observed via the large hysteresis between its adsorption and desorption isotherms. Carbon-based sorbents are an interesting alternative to MOFs due to their simpler synthesis processes and higher scalability potential [21], [22]. Legrand et al. recently described nanoporous sponges (NPS) sorbents made of pyrolyzed resorcinol-formaldehyde resin and eventually functionalized with oxygen through air oxidation [23]. This carbon-based sorbent exhibited lower water uptakes than MOFs and silica gel with values ranging from 0.14 kg/kg in its native state to 0.3 kg/kg when functionalized, though on-going work aims to improve these performance. Indeed, Huber *et al.* described methods to improve the water uptake of such materials up to 0.5 kg/kg with different types of treatment, including CO_2 and KOH activation [24]. NPS energy requirements have however yet to be thoroughly characterized.

Thermal management has been described by Lapotin *et al.* to be a limiting factor in an actual water capture system [25]. Water adsorption is an exothermic process, and the released heat can affect the adsorption performance. Several solutions have been proposed in the literature, including the dispersion of sorbents in metal foams to promote heat dissipation, or the use of dual stage systems, where the heat of adsorption is used to desorb water from a subsequent compartment [25], [26]. Thus, it appears important to better understand the fundamental thermodynamic properties of

sorbents to improve the thermal management in water capture set-ups. Herein, five sorbents representing carbon-based materials (NPS and O-NPS), silica gel (type A) and MOFs (MOF-801-P and Cr-MIL-101) are studied to assess their thermodynamic properties that, despite being necessary variables, are generally ignored in atmospheric water capture studies. To do so, we applied an innovative method where the thermodynamic data are extracted from the isotherms at three specific temperatures. These properties include (i) Gibbs free energy, linked to the spontaneity of the adsorption process and the hygroscopicity of the sorbents, (ii) differential and integral enthalpy, representing the energy released during the exothermic adsorption process, and (iii) differential and integral entropy, being the distribution of energy in possible microscopic states. In other terms, entropy corresponds to how the energy is dispersed in the overall system when new water molecules are adsorbed, and insight about the interactions between water molecules and the sorbent surface can thus be derived. One of the objectives of the present study was to determine if our carbon-based sorbents could thermodynamically compete with sorbents reported to have higher water uptake.

2. Materials and methods

2.1. Sorbent materials

The thermodynamic properties are assessed for five samples. They consist of nanoporous sponges (NPS), oxidized nanoporous sponges (O-NPS), silica gel and two metal-organic frameworks (MOFs): MOF-801-P and Cr-MIL-101. NPS are synthesized from the pyrolysis of resorcinol-formaldehyde resin and their characterization was described in details in Legrand *et al.* [23]. O-NPS were obtained by oxidizing the NPS sample in air atmosphere at 700 °C for 1h. Silica gel (type A, Dry-Packs®) was purchased from Amazon. Finer powders of silica gel were obtained by

grinding of the gel beads for 20 s in a Simplicite automatic grinder. Cr-MIL-101 and MOF-801-P were respectively chromium- and zirconium-based MOFs that were already described in literature [27]–[30]; both were purchased from Nanoshel-UK LTD.

2.2. Environmental chamber

Water adsorption isotherms were measured for each sorbent, at three temperatures: 25, 30 and 35 °C. The measurement of these isotherms was performed in a custom-made and fully automated environmental chamber, depicted in Figure S1, employing a gravimetric method. In this method, the weight of the sample is continuously measured while the relative humidity varies and the temperature remains constant. The A sample of 3-5 g sorbent is dispersed on a thin layer in a 71 cm^2 glass dish suspended under an AB204-S analytical balance from Mettler Toledo. Relative humidity (RH) was controlled by a humidifier and a solenoid valve connected to a dry air inlet. Temperature was controlled with a heater for the duration of the experiment. Also, a fan kept the conditions homogeneous in the entire volume of the environmental chamber. Both humidifier, solenoid valve, heater and fan were controlled by an Arduino via a Python interface. Prior to isotherm measurement, the samples were left to dry in the environmental chamber for several hours until mass equilibration was reached. The adsorption isotherm protocol involved increasing the RH in 5 % steps from 5 to 95 % RH, and each step was maintained (1-4 h) until the sorbent mass could equilibrate.

2.3. Thermodynamic equations

Water adsorption isotherms were fitted applying the Stineman's algorithm [31] using the KaleidaGraph 4.5 (Synergy) software package. This fitting allowed extrapolating 100 data points based on the experimental isotherms. Gibbs molar free energy was estimated using Equation 1:

$$\Delta G = RT\ln(a_w) \qquad \text{(Equation 1)}$$

where T [K] is the absolute temperature, R [J/mol·K] is the universal gas constant and a_w (= RH/100) [-] is the water activity.

To calculate the differential enthalpy or isosteric heat, the methodology reported by Flores-Andrade *et al.* was applied [32]. First, Othmer's equation (Equation 2) was used to determine the changes in differential enthalpy at the water-solid interface at different stages of adsorption [33]:

$$ln(P_v) = \left(\frac{H_v(T)}{H_v^0(T)}\right)_M lnP_v^0 + C_1 \qquad \text{(Equation 2)}$$

Where M [g H_2O/100 g dry sorbent] is the air moisture, $H_v(T)$ [J/mol] is the isosteric heat for water sorption, $H_v^0(T)$ [J/mol] is the heat of condensation for pure water and C_1 is a constant of adsorption, P_v [Pa] is the partial vapor pressure of water in the system and P_v^0 [Pa] is the standard state vapor pressure. By plotting $ln(P_v)$ vs. $ln(P_v^0)$, a straight line can be obtained if the ratio $H_v(T)/H_v^0(T)$ is constant for the studied range of temperature. The differential adsorption molar enthalpy ΔH_{diff} [J/mol] or net isosteric heat of adsorption was then computed with Equation 3:

$$\left(\Delta H_{diff}\right)_T = \left(\frac{H_v(T)}{H_v^0(T)} - 1\right)_M H_v^0(T) \qquad \text{(Equation 3)}$$

The differential enthalpy values previously calculated were used to calculate the change in the molar differential entropy ΔS_{diff} [J/mol], following the methodology reported by Flores-Andrade *et al.* [32] using Equation 4:

$$\left(\Delta S_{diff}\right)_T = -\frac{\left(\Delta H_{diff}\right)_T}{T} - Rlna_w \qquad \text{(Equation 4)}$$

The molar integral enthalpy $(\Delta H_{int})_T$ [J/mol] was calculated by maintaining diffusion pressure (ϕ) constant, as reported by Flores-Andrade *et al.* [32] using Equation 5. The diffusion pressure is the available work to adsorb humidity. Rowley and Innes defined it as the total reversible work involved in the formation of an interface between the condensed water and the gas [34].

$$(\Delta H_{int})_T = \left(\frac{H_{v,int}(T)}{H_v^0(T)} - 1\right)_\phi H_v^0(T) \qquad \text{(Equation 5)}$$

where $H_{v,int}(T)$ [J/mol] is the integral molar heat of water adsorbed in the material, $H_v^0(T)$ [J/mol] is the heat of condensation for pure water and can by determined with the Wexler equation (Equation 6), valid between 0 and 100 °C [35]:

$$H_v^\circ(T) = 6.15X10^4 - 94.14T + 17.74x10^{-2}T^2 - 2.03x10^{-4}T^3 \quad \text{(Equation 6)}$$

The diffusion pressure ϕ can be found via Equations 7 and 8:

$$\phi = \mu_{ap} - \mu_a = RT\frac{W_{ap}}{W_v}\int_0^{a_w} Mdln(a_w) \qquad \text{(Equation 7)}$$

$$\phi = \alpha_1 T\int_0^{a_w} Mdln(a_w) \qquad \text{(Equation 8)}$$

where μ_{ap} [J/mol] is the chemical potential of the pure adsorbent, μ_a [J/mol] is the chemical potential of the adsorbent in the condensed phase, W_{ap} [kg/mol] is the molecular weight of the adsorbent, and W_v [kg/mol] is the molecular weight of water.

The changes in the molar integral entropy $(\Delta S_{int})_T$ [J/mol] were calculated as reported by Pascual-Pineda *et al.* and Acosta-Domínguez *et al.* in Equation 8 [36], [37]:

$$(\Delta S_{int})_T = S_1 - S_L = -\frac{(\Delta H_{int})_T}{T} - Rln(a_w) \qquad \text{(Equation 8)}$$

where $S_I = S/N_I$ [J/mol·K] is the integral entropy of the water adsorbed; S [J/ K] is the total entropy of water adsorbed in the adsorbent; N_I [mol] is the moles of water adsorbed in the adsorbent, and S_L [J/mol·K] is the molar entropy of the pure liquid water in equilibrium with the vapor.

3. Results and discussion

3.1. Sorbent surface chemistry

The five studied sorbents presented various surface chemistry and physical properties and were thus expected to have different thermodynamic properties (Table 1). Simplified surface chemistry is illustrated in Figure 1.

Table 1: Physical properties and surface chemistry of the sorbents.

Sorbent	Silica gel [38], [39]	NPS [23]	O-NPS [23]	Cr-MIL-101 [40], [41]	MOF-801-P [40], [42]
Surface area (m^2/g)	650	487	484	990	1300
Pore size (nm)	2.2	1.5	1.7	2.0	0.5
XPS composition (at%)	Si: 33.3 O: 66.7	C: 93.8 O: 6.2	C:93.0 O: 7.0	C: 48.9 O: 33.1 Cr: 18.0	C: 20.3 O: 45.1 Zr: 34.6
Estimated –OH concentration (-OH/nm^2)	3.1	0.5	0.8	1.5	1.8

Silica gel can be considered as a polymeric form of silicic acid in an amorphous network of SiO_4 tetrahedra. The surface is terminated by either siloxane (-Si-O-Si-) or silanol groups (-Si-OH) and thus exhibits high oxygen concentration, rendering it hydrophilic [43]. In average, 3.1 –OH groups per nm^2 are present on the surface with irregular distribution [44]. For the rest of the sorbents, the hydroxyl surface concentration was estimated based on available atomic O concentration from XPS, and surface area measurement from BET. NPS and O-NPS were derived from the pyrolysis of resorcinol-formaldehyde resin pyrolysis (with an oxidation step added for O-NPS) and thus are mostly composed of carbon sp2, with slightly more oxygen for O-NPS compared to NPS. Among the oxygen moieties contained on the carbon-based sorbents, -OH groups were identified as primary adsorption sites using the Do & Do model [23]. NPS and O-NPS contained respectively 0.5 and 0.8 –OH groups per nm^2. Cr-MIL-101 was synthesized from $Cr(NO_3)_3 \cdot 9H_2O$ salt and trimesic acid. The resulting sorbent material contained a high oxygen concentration on its surface. However, most of these oxygen atoms were involved in the MOF structure where they were linked to Cr atoms, and thus only a few oxygen atoms from carboxylic moieties would be able to

participate in the water adsorption. From surface analysis data in [28], [41], it was estimated there were 1.5 –OH groups per nm^2. Many derivatives of Cr-MIL-101 could be found in the literature by functionalizing the organic linkers with various groups such as $–NH_2$, $-NO_2$ or SO_3H [28]. MOF-801-P was synthesized from $ZrOCl_2 \cdot 8H_2O$ salt and fumaric acid. Similarly to Cr-MIL-101, most oxygen atoms participated in the MOF structure, and it was estimated that only 1.8 –OH groups per nm^2 were available for water adsorption.

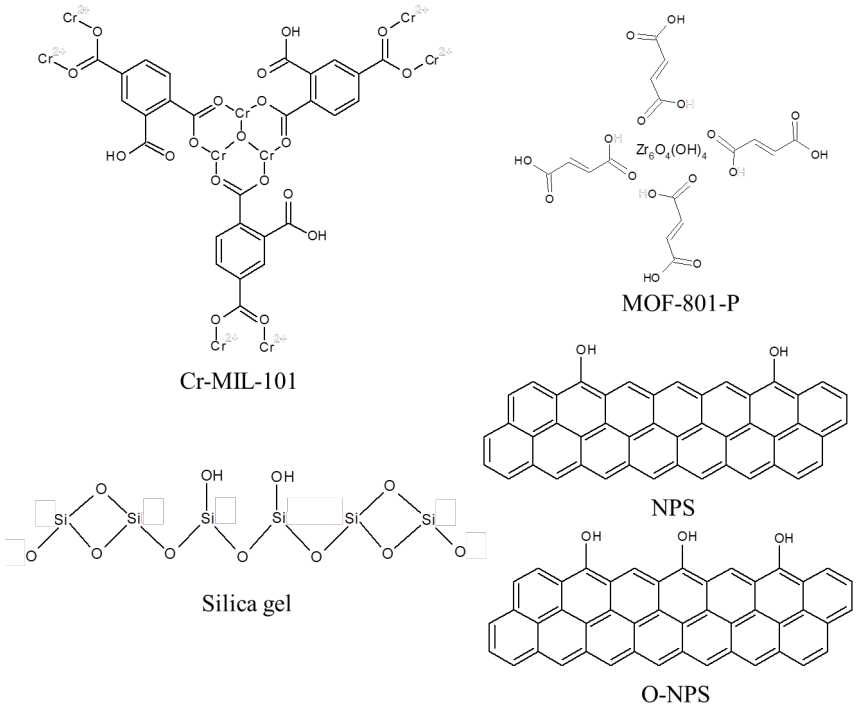

Figure 1: Simplification of the surface chemistry of the different studied sorbents to illustrate various oxygen concentration. NPS and O-NPS structure is idealized since it contains more than 90% of sp2 carbon.

Adsorption isotherms at 30 °C for the five studied sorbents are presented in Figure 2 (with hysteresis shown in Figure S2 and isotherms at 25 °C, 30 °C and 35 °C shown in Figure S3). NPS and silica gel exhibited decreasing equilibrium moisture content when increasing temperature at constant water activity due to the exothermic nature of the adsorption process [35]. O-NPS, MOF-

801-P and Cr-MIL-101 had several regions of the isotherms where the opposite phenomenon was observed, and the equilibrium water constant increased with increasing temperature.

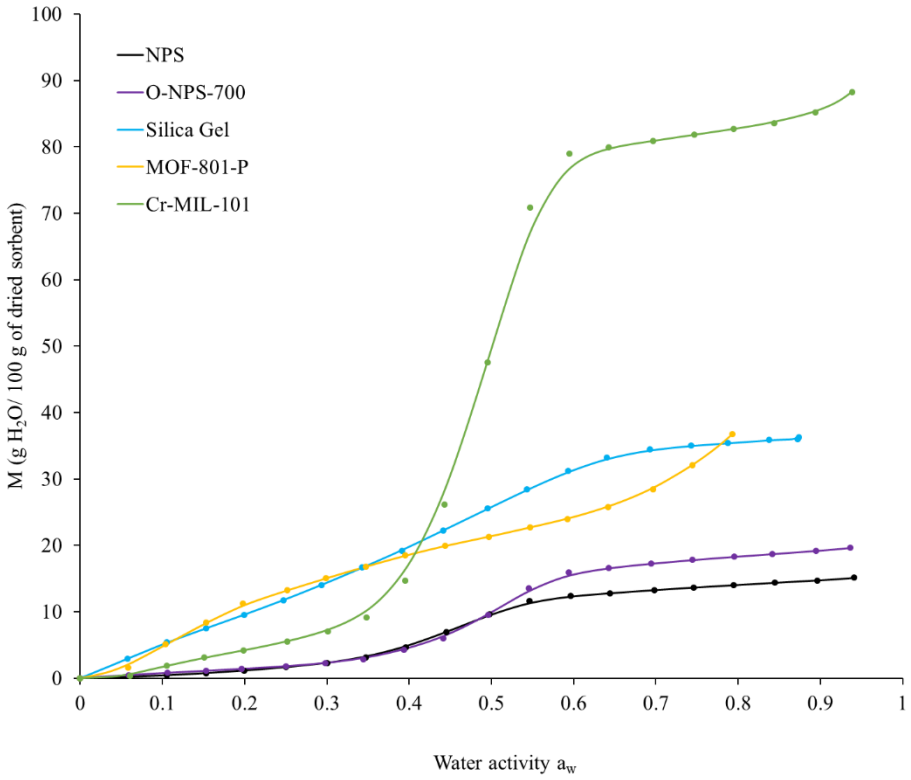

Figure 2: Summary of the adsorption isotherms measured at 30 C for the studied sorbents. The experimental points are fitted with the Stineman's algorithm, represented by the continuous line.

NPS, O-NPS and Cr-MIL-101 isotherms presented a type V shape, according to the classification proposed by the International Union of Pure and Applied Chemistry (IUPAC); this is an S-shaped isotherm commonly found on various charcoals, carbon black and more generally hydrophobic materials [45]. Non-porous carbons with a void or small presence of Oxygen Functional Groups (OFGs) such as graphite or Graphitized Carbon Black (GCB) would present a Type III isotherm instead [45]. Silica gel was in good agreement with the experimental isotherms from literature [38]. However, it was observed that the isotherm from the commercial MOF-801-P deviated from literature reports, especially at low water activity, where the isotherms from literature exhibit a

sharp increase [17]. Due to the constituency and adequacy of the other isotherms, it was concluded that this behavior came from the sample itself, and that scale-up of the MOF-801-P sorbent synthesis might have altered its adsorption properties.

3.2. Gibbs free energy

Gibbs free molar energy of the different sorbents are shown in Figure 3 as a function of moisture (M, g H_2O / 100 g of dried sorbent) (available at other temperatures in Figure S4). Free energy increased with increasing water activity; thus, the process was less spontaneous as the sorbent moisture increased. It was also observed that at low moisture content and with increasing temperature, adsorption was less spontaneous since more energy was required for adsorption to occur [5]. At higher moisture, the reverse phenomenon happened for sorbents that had higher water uptakes at higher temperatures.

Gibbs free energy was also used to compare the hygroscopicity of the sorbents, i.e. the facility for a sorbent to adsorb water vapor from its surrounding environment. The lowest energy values were correlated to the most hygroscopic materials. Silica gel appeared to be the most hygroscopic material, followed by the two MOFs, Cr-MIL-101 and MOF-801-P and then the carbon-based samples, NPS and O-NPS. This behavior aligns with the –OH concentration on the sorbents' active surface area, and more generally with the surface chemistry. Both NPS and O-NPS samples reached a "plateau" rapidly at around -2000 J/mol during the adsorption process, which suggested that water was adsorbed with homogenous spontaneity over a considerable range of relative humidity.

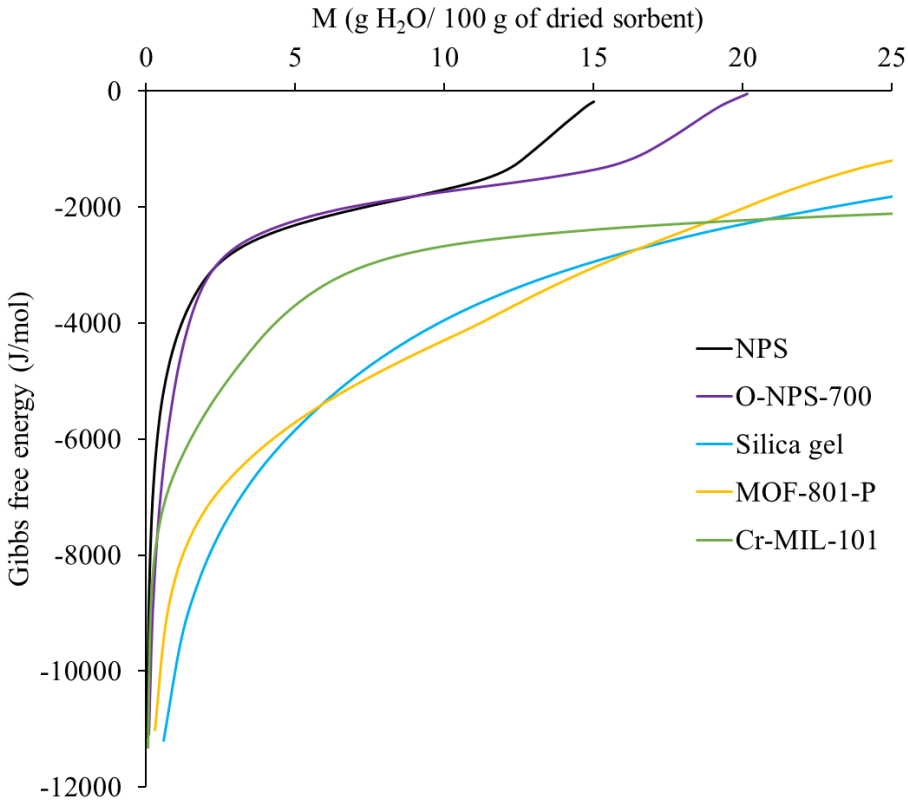

Figure 3: Gibbs free energy of the sorbents based on their moisture content. The x-axis was stopped at 25 g H_2O/ 100 g of dried sorbent because most thermodynamic information was contained at low moisture content.

3.3. Enthalpy of adsorption

The net isosteric heat of adsorption or differential enthalpy at 30 °C are presented in Figure 4, while temperature dependent graphs are available in Figure S5. At low water activities, the differential enthalpy was higher than the enthalpy of vaporization of pure water for all the samples, indicating that the interactions between the water molecules and the surface of the sorbent material were higher than the intermolecular forces of water molecules in the liquid state (bulk). It was observed that the net isosteric heat of adsorption decreased exponentially when increasing the water activity, evidence that the highly active sites (-OH groups) were being occupied as adsorption process evolves. After that, differential enthalpy slightly oscillated close to the reference (pure water), meaning that the enthalpy of adsorption was practically the same as the

heat of vaporization of water at each specific temperature (~44 kJ/mol). Liu *et al.* (2017) concluded that during the main pore filling in porous carbons, the isosteric heat was close to the heat of condensation because the water adsorption was governed by water-water interactions [44]. One should note that the NPS sample presented an equivalent behavior to the commercial Cr-MIL-101 adsorbent, i.e., relatively low water-absorbent interactions when compared to silica gel and MOF-801-P. The weak interactions on the NPS and O-NPS became advantageous for water harvesting applications since less energy would be required to dry the sorbent before using it again in a cyclical adsorption-desorption process.

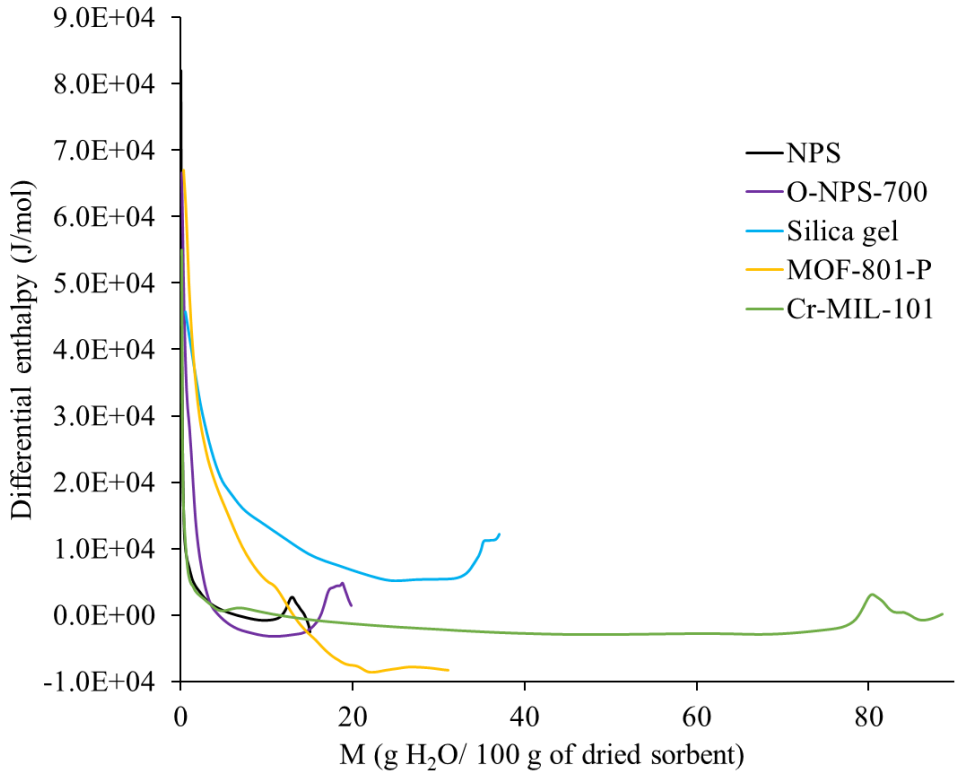

Figure 4: Net isosteric heat of adsorption depending on the moisture content for the different sorbents.

The integral enthalpy of the different sorbents at 30 °C are shown in Figure 5 (temperature dependence is given in Figure S6). This property represents the average energetic state of the adsorbed water on the surface of the material. That is, the average interactions between water

molecules and adsorbent at a specific moisture content [31]. Integral enthalpy was directly correlated to the amount of energy released during water adsorption. The highest amount of energy was released for the first water molecules being adsorbed, which had the highest water-sorbent interaction. This behavior could be employed to better understand energy release during the adsorption step and optimize the energy management in a water capture set-up, where heat was demonstrated to be a limiting step in certain cases [25], [26].

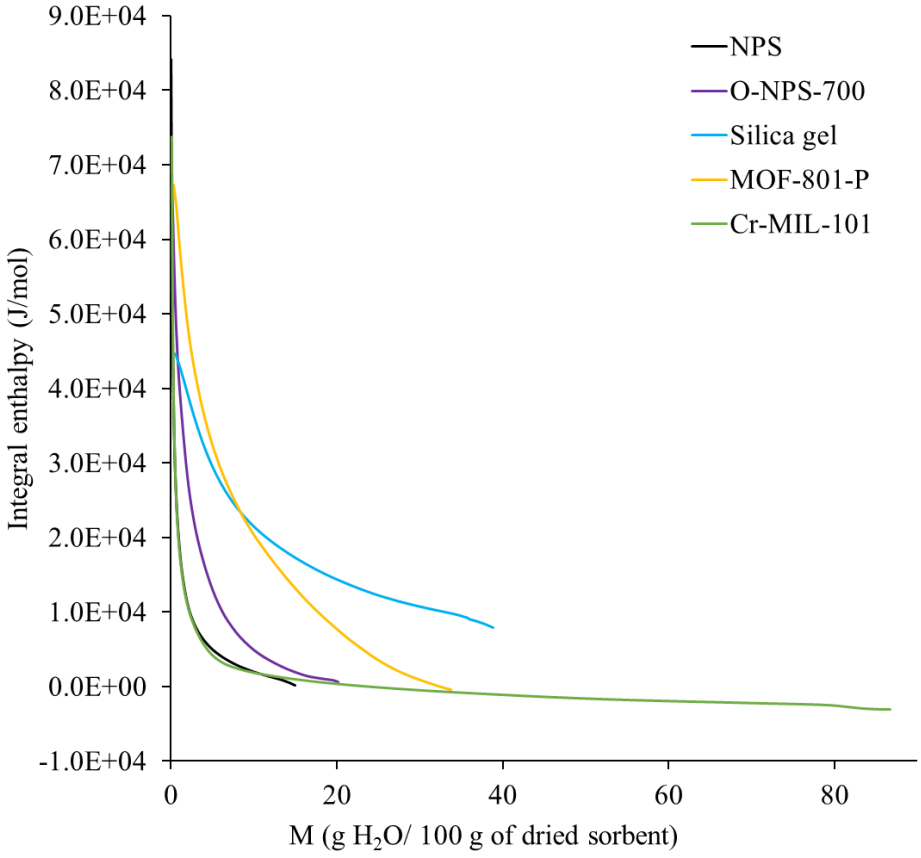

Figure 5: Integral enthalpy of adsorption of the sorbents. The y-axis origin corresponds to the heat of vaporization of pure water at 30 °C.

The moisture content was defined as a percentage of the maximum water uptake $\%M_{max}$. For example, 30 $\%M_{max}$ of silica gel would correspond to 11.5 $g_{H2O}/100\ g_{sorbent}$. Taking into account the heat of vaporization for pure water at 30 °C, adsorbing water from 0 $\%M_{max}$ to 30 $\%M_{max}$ for

silica gel would release an average energy of 63.5 kJ/mol, compared to 51.5 kJ/mol to adsorb water from 0 $\%M_{max}$ (dry sorbent) to 100 $\%M_{max}$, due to high water-adsorbent interaction at low moisture content. The summary of the released heat of adsorption for different cases applied on all sorbents was shown in Table 2. These simple cases show that the samples with the lowest water-sorbent interactions at higher water activity, i.e. NPS and Cr-MIL-101, released lower amounts of energy than silica gel and MOF-801-P that have higher water-sorbent interactions. In other words, the amount of energy released during the adsorption, and by analogy the required energy for desorption, could be controlled in an actual water capture set-up by setting the moisture content levels during cycles of adsorption-desorption. O-NPS was considered as an intermediate in terms of water-sorbent interactions between NPS and Cr-MIL-101 on one side and silica gel and MOF-801-P on the other side.

Table 2: Heat of adsorption released during three adsorption cases for the sorbents.

Sorbent	Heat of adsorption for 0 $\%M_{max} \rightarrow 10$ $\%M_{max}$ (kJ/mol)	Heat of adsorption for 0 $\%M_{max} \rightarrow 30$ $\%M_{max}$ (kJ/mol)	Heat of adsorption for 0 $\%M_{max} \rightarrow 100$ $\%M_{max}$ (kJ/mol)
NPS	57.5	49.3	43.8
O-NPS	71.5	54.0	44.3
Silica gel	75.9	63.5	51.5
MOF-801-P	81.1	63.7	43.2
Cr-MIL-101	45.8	43.4	40.6

The enthalpy of adsorption for silica gel has already been characterized in literature. Chakraborty *et al.* determined that silica gel type RD had an enthalpy of adsorption at 30 °C of 2,550 kJ/kg, i.e.

46.0 kJ/mol [47]. Ng *et al.* reported a value of 2,380 kJ/kg, i.e. 42.8 kJ/mol for silica gel type 3A [48] and 45.2 kJ/mol for silica gel type RD. Chua *et al.* reported values of 48.8 and 48.5 kJ/mol for silica gel of respectively type A and type RD [49]. The enthalpy of adsorption varied from a silica gel type to another, but variations were also observed for the same type of silica gel, depending on the studies. It appeared that the present study slightly overestimated the enthalpy of adsorption compared to available literature data. Explanations for this could include the material itself, purchased from large-scale commercial supplier, and experimental errors that make difficult the precise determination of moisture content at low water activity and potentially causing variations in the thermodynamic properties. Enthalpy of adsorption was also studied in literature for MOF-801-P. Kim *et al.* determined values of 55 kJ/mol for this sorbent at 30 °C [50] while Furukawa *et al.* reported enthalpy of adsorption of 60 kJ/mol at similar temperature [16]. While the present study reported a lower value, it appeared more delicate to compare our value with literature since the isotherm shape measured here greatly differed from those studies.

3.4. Entropy

Differential and integral entropy are respectively presented in Figure 6 and 7. Statistical thermodynamics describes entropy as the distribution of the system energy in a number of possible microscopic states at thermodynamic equilibrium [51]. Applied to water adsorption, entropy corresponds to the energy spreading or dispersing by adsorbed water molecules, and the impact of intermolecular interaction between the water molecules and the sorbent surface on the energy dispersal within the system. It is important to point out that the differential adsorption molar entropy does not represent the energy spreading of the entire system, instead it shows the contribution to the energy spreading when the last molecules of water are adsorbed at a specific water level [31]. As such, this property allows us to determine the water content for which new

arriving molecules do not affect the energy spreading of the system for each sample. This is valuable information for the design and scale-up of sorbent technologies for water recovery since it allows to predict the minimal drying conditions for the sorbent before it is used again to absorb water in a cyclical system. Indeed, new arriving water molecules that do not contribute to the energy spreading would practically arrange in an equivalent way as they would do in pure water. This implies that extraction conditions will then be equivalent as in pure water. An equivalent shape or behavior of the differential entropy has been observed in a MOF [52]. It can be observed that, for the NPS and the Cr-MIL-101 samples, differential entropy rapidly reaches a value of 0, indicating that additional molecules of water being adsorbed become equal to the molar entropy of liquid water in equilibrium with gaseous water. Even though the energy dispersal for the MOF-801-P sample is affected at low water contents, it also becomes stable close to 0 at around 13 g H_2O/100 g of MOF-801-P. Silica gel was the sample where the energy dispersal is least affected by the new arriving molecules due to the higher energy sites and higher water-sorbent interactions.

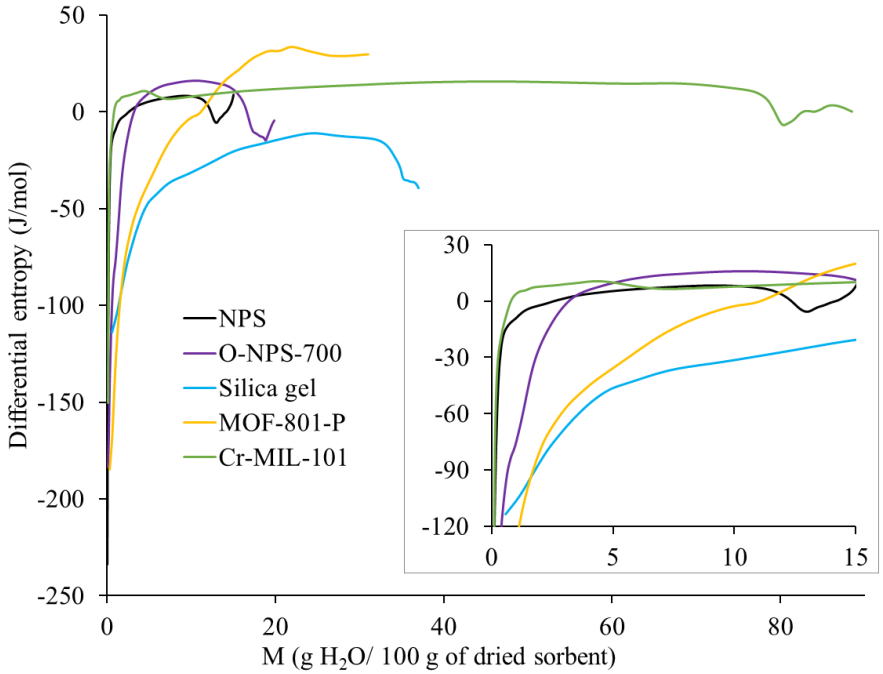

Figure 6: Differential entropy of the sorbents and enhanced view of the low moisture content region.

Integral entropy represents the average entropy of the entire system and is shown in Figure 7. This property is defined as the integral entropy of the water in the adsorbed state minus the molar entropy of the pure liquid water in equilibrium with the vapor (S_I-S_L). It then allows us to observe that, for most of the sorbent the adsorption process, the energy of the water molecules spreads in an equivalent way as it would in pure liquid water. Overall, NPS and Cr-MIL-101 saw their entropy rapidly converge to 0, showing the energy of the adsorbed water rapidly reached the same distribution of microscopic states than pure water. The integral entropy of MOF-801-P, also converged towards 0, but the water molecules remained in a lower energy dispersal before fully filling the sorbent. Water molecules in silica gel did not reach the entropy of pure water and the strong interactions with sorbent surface maintained a lower energy dispersal. This also shows that it is entropically advantageous to adsorb water up to the maximum uptake, especially for NPS and Cr-MIL-101. It is shown that it is not necessary to completely dry the samples before using it again in a cyclical process since a more negative entropy is correlated with higher difficulty to remove

them from the sorbent. From a practical point of view, this implies that NPS and Cr-MIL-101 should maintain a moisture content of 3-5 g_{H2O}/100g of dried sorbent between cycles to ensure that the system keeps an entropy close to that of pure water. This conditions could be achieved by performing adsorption-desorption steps with a lower limit at 20-35%RH.

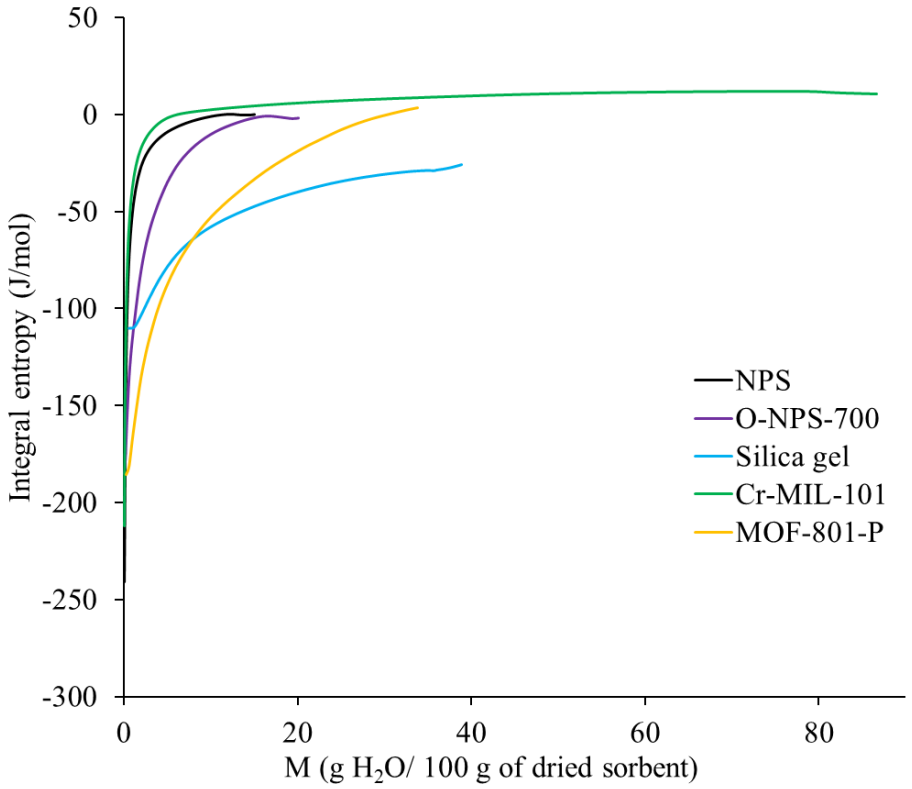

Figure 7: Integral entropy of the sorbents. The y-axis origin corresponds to the entropy of pure water at 30 °C.

The five studied sorbents exhibited various levels of –OH concentration on their active surface area, as shown in Table 1 [23]. The different thermodynamic properties were correlated with these surface chemistries. Gibbs free energy confirmed the hygroscopicity of the sorbents. At low relative humidity, the carbon-based sorbents, NPS and O-NPS were the least hygroscopic samples while silica gel had the highest hygroscopicity. In terms of integral enthalpy, the sorbents with the lowest –OH surface concentration had the highest enthalpy adsorption at low moisture content, due to a higher water-sorbent interaction. However, the adsorption enthalpy for these samples

converged more rapidly towards the heat of vaporization of pure water than for the samples with higher water-sorbent interactions. Similar trends were observed with the integral entropy, where NPS, O-NPS and Cr-MIL-101 had lower values of entropy at low moisture content, indicating a higher number of possible microscopic states of the first adsorbed molecules. The integral entropy of these samples was converged rapidly towards 0, equivalent of the entropy of pure water. In contrary, silica gel and MOF-801-P kept lower integral entropies for higher moisture content, due a higher water-sorbent interaction and preventing the dominance of water-water interactions.

Despite a general good agreement between the –OH concentration and thermodynamic behaviors, some discrepancies were still observed for enthalpy and entropy, and especially with Cr-MIL-101 that had a lower enthalpy and higher entropy at low moisture content compared to O-NPS. This phenomenon was representative that water adsorption was a more complex phenomenon, and several additional parameters should be considered. For example, even if –OH groups were identified as primary adsorption sites for NPS and O-NPS, surface chemistry could be more complex with other moieties having various repulsive or attractive behavior towards water. On top of the surface chemistry, water adsorption also depends on the pore size and geometry. For example, sudden variations in the pore diameter could locally lead to pore blocking, one of the potential causes for hysteresis between adsorption and desorption [53]. The present work focused mainly on the thermodynamic properties of the sorbent during the adsorption step. While hysteresis during desorption is likely to affect the thermodynamic behavior of the sorbent, one should expect only minor differences between adsorption and desorption integral properties. This is because the thermodynamic properties of interest are mainly extracted in the low humidity region (water activity = 0 – 0.2) where the sorbent surface – water molecules interactions are the strongest and the hysteresis is minimal (Figure S2).

4. Conclusion

The thermodynamic properties of five sorbents (Cr-MIL-101, MOF-101, silica gel, NPS and O-NPS) have been assessed based on the adsorption isotherms at three temperatures. Thermodynamic properties of silica gel were in good agreement with those found in literature. Gibbs free energy gave insight on the spontaneity of the adsorption process and on the hygroscopicity of the sorbents surface, that was correlated with the surface chemistry and more specifically the –OH surface concentration. Enthalpy of adsorption demonstrated that the highest amount of released energy occurred for the first adsorbed water molecules that had the highest water-sorbent interaction. The changes of adsorption enthalpy between the analyzed sorbents could be mostly correlated with the surface chemistry; other parameters could potentially affect the thermodynamic properties, such as pore size distribution and surface heterogeneity, whose effect should be studied in future. Based on the enthalpy of adsorption, it could be possible to optimize the amount of released energy by performing incomplete desorption between adsorption steps, and particularly for the most hydrophobic sorbents, namely NPS and Cr-MIL-101. Entropy provided information on the distribution of microscopic states in adsorbed water molecules, i.e. which is related to the energy spreading or dispersing within the system. While the most hydrophobic sorbents rapidly reached a similar entropy to that of pure liquid water, silica gel maintained a lower entropy due to higher water-sorbent interactions. It showed that it was entropically advantageous to entirely use the materials to adsorb water and set conditions to avoid complete desorption. A narrow temperature range suitable for atmospheric water capture was studied in the present work. Future work should extend the study of the thermodynamic properties to wider temperature range (10-50 °C) to simulate the harsher conditions that can be found in the desert, for example.

5. Acknowledgements

The authors acknowledge financial support from the Natural Sciences and Engineering Research Council of Canada (NSERC grant CRD-522391), Prima (grant R16-46-003), Mitacs (IT16469) and Awn Nanotech Inc.

6. Conflict of interest

The authors U. Legrand, J. R. Tavares and R. Boudreault have filed a patent on the NPS sorbents, and thus acknowledge their personal financial interest in this research. R. Boudreault is the CEO of Awn Nanotech Inc. the industrial partner supporting this research. This potential conflict of interest has not led any of the co-authors to bias or otherwise modify any of the methods and/or results reported here.

7. References

[1] Statistics Canada, “Human Activity and the Environment,” 2011. doi: 10.2307/3549992.

[2] The World Bank, “CIWA Annual Report Fy 2020,” 2020.

[3] J. Grabinsky and C. Borja-Vega, “World Statistics Day: Five key statistics on global access to water, sanitation and hygiene,” 2020. https://blogs.worldbank.org/water/world-statistics-day-five-key-statistics-global-access-water-sanitation-and-hygiene (accessed Jul. 29, 2021).

[4] H. Chang, *Water and Climate Change*. 2019.

[5] T. Hrdinka, O. Novický, E. Hanslík, and M. Rieder, “Possible impacts of floods and droughts on water quality,” *J. Hydro-Environment Res.*, vol. 6, no. 2, pp. 145–150, 2012, doi: 10.1016/j.jher.2012.01.008.

[6] E. Jones, M. Qadir, M. T. H. van Vliet, V. Smakhtin, and S. mu Kang, “The state of

desalination and brine production: A global outlook," *Sci. Total Environ.*, vol. 657, no. December 2018, pp. 1343–1356, 2019, doi: 10.1016/j.scitotenv.2018.12.076.

[7] N. Ahmad and R. E. Baddour, "A review of sources, effects, disposal methods, and regulations of brine into marine environments," *Ocean Coast. Manag.*, vol. 87, pp. 1–7, 2014, doi: 10.1016/j.ocecoaman.2013.10.020.

[8] A. Grosman and C. Ortega, "Capillary condensation in porous materials. Hysteresis and interaction mechanism without pore blocking/percolation process," *Langmuir*, vol. 24, no. 8, pp. 3977–3986, 2008, doi: 10.1021/la703978v.

[9] T. Horikawa, D. D. Do, and D. Nicholson, "Capillary condensation of adsorbates in porous materials," *Adv. Colloid Interface Sci.*, vol. 169, no. 1, pp. 40–58, 2011, doi: 10.1016/j.cis.2011.08.003.

[10] A. J. Rieth, S. Yang, E. N. Wang, and M. Dincă, "Record Atmospheric Fresh Water Capture and Heat Transfer with a Material Operating at the Water Uptake Reversibility Limit," *ACS Cent. Sci.*, vol. 3, no. 6, pp. 668–672, 2017, doi: 10.1021/acscentsci.7b00186.

[11] S. Inoue, N. Ichikuni, T. Suzuki, T. Uematsu, and K. Kaneko, "Capillary condensation of N2 on multiwall carbon nanotubes," *J. Phys. Chem. B*, vol. 102, no. 24, pp. 1–4, 1998, doi: 10.1021/jp973319n.

[12] D. Wallacher, N. Künzner, D. Kovalev, N. Knorr, and K. Knorr, "Capillary condensation in linear mesopores of different shape," *Phys. Rev. Lett.*, vol. 92, no. 19, pp. 1–4, 2004, doi: 10.1103/PhysRevLett.92.195704.

[13] D. D. Do, S. Junpirom, and H. D. Do, "A new adsorption-desorption model for water adsorption in activated carbon," *Carbon*, vol. 47, no. 6, pp. 1466–1473, 2009, doi: 10.1016/j.carbon.2009.01.039.

[14] S. Furmaniak, P. A. Gauden, A. P. Terzyk, G. Rychlicki, R. P. Wesołowski, and P. Kowalczyk, "Heterogeneous Do-Do model of water adsorption on carbons," *J. Colloid Interface Sci.*, vol. 290, no. 1, pp. 1–13, 2005, doi: 10.1016/j.jcis.2005.07.043.

[15] M. Neitsch, W. Heschel, and M. Suckow, "Water vapor adsorption by activated carbon: A modification to the isotherm model of Do and Do," *Carbon*, vol. 39, no. 9, pp. 1437–1438, 2001, doi: 10.1016/S0008-6223(01)00077-X.

[16] H. Furukawa *et al.*, "Water adsorption in porous metal-organic frameworks and related materials," *J. Am. Chem. Soc.*, vol. 136, no. 11, pp. 4369–4381, 2014, doi: 10.1021/ja500330a.

[17] S. Kim, Hyunho, Yang *et al.*, "Water harvesting from air with metal-organic frameworks powered by natural sunlight," *Science*, vol. 434, no. April, pp. 430–434, 2017.

[18] B. S. Gelfand and G. K. H. Shimizu, "Parameterizing and grading hydrolytic stability in metal-organic frameworks," *Dalt. Trans.*, vol. 45, no. 9, pp. 3668–3678, 2016, doi: 10.1039/c5dt04049c.

[19] M. Rubio-Martinez, C. Avci-Camur, A. W. Thornton, I. Imaz, D. Maspoch, and M. R. Hill, "New synthetic routes towards MOF production at scale," *Chem. Soc. Rev.*, vol. 46, no. 11, pp. 3453–3480, 2017, doi: 10.1039/c7cs00109f.

[20] X. Zhou, H. Lu, F. Zhao, and G. Yu, "Atmospheric Water Harvesting: A Review of Material and Structural Designs," *ACS Materials Lett.*, vol. 2, no. 7 pp. 671-684, 2020, doi: 10.1021/acsmaterialslett.0c00130.

[21] G. P. Hao *et al.*, "Unusual ultra-hydrophilic, porous carbon cuboids for atmospheric-water capture," *Angew. Chemie - Int. Ed.*, vol. 54, no. 6, pp. 1941–1945, 2015, doi: 10.1002/anie.201409439.

[22] L. Huber *et al.*, "Monolithic nitrogen-doped carbon as a water sorbent for high-performance adsorption cooling," *RSC Adv.*, vol. 6, no. 30, pp. 25267–25278, 2016, doi: 10.1039/c6ra00548a.

[23] U. Legrand *et al.*, "Nanoporous sponges as carbon-based sorbents for atmospheric water generation," *Ind. Eng. Chem. Res.*, vol. 60, no. 35, pp. 12923-12933, 2021, doi: 10.1021/acs.iecr.1c02248.

[24] L. Huber *et al.*, "Water sorption behavior of physically and chemically activated monolithic nitrogen doped carbon for adsorption cooling," *RSC Adv.*, vol. 6, no. 84, pp. 80729–80738, 2016, doi: 10.1039/c6ra18660b.

[25] A. LaPotin, H. Kim, S. R. Rao, and E. N. Wang, "Adsorption-Based Atmospheric Water Harvesting: Impact of Material and Component Properties on System-Level Performance," *Acc. Chem. Res.*, vol. 52, no. 6, pp. 1588–1597, 2019, doi: 10.1021/acs.accounts.9b00062.

[26] A. LaPotin *et al.*, "Dual-Stage Atmospheric Water Harvesting Device for Scalable Solar-Driven Water Production," *Joule*, vol. 5, no. 1, pp. 166–182, 2021, doi: 10.1016/j.joule.2020.09.008.

[27] B. Tan *et al.*, "Mixed-Solvothermal Synthesis of MIL-101(Cr) and Its Water Adsorption/Desorption Performance," *Ind. Eng. Chem. Res.*, vol. 58, no. 8, pp. 2983–2990, 2019, doi: 10.1021/acs.iecr.8b05243.

[28] N. Ko *et al.*, "Tailoring the water adsorption properties of MIL-101 metal-organic frameworks by partial functionalization," *J. Mater. Chem. A*, vol. 3, no. 5, pp. 2057–2064, 2015, doi: 10.1039/c4ta04907a.

[29] H. Kim *et al.*, "Water harvesting from air with metal-organic framework powered by

natural sunlight," *Science*, vol. 434, no. April, pp. 430–434, 2017, doi: 10.1126/science.aam8743.

[30] H. Kim *et al.*, "Adsorption-based atmospheric water harvesting device for arid climates," *Nat. Commun.*, vol. 9, no. 1, pp. 1–8, 2018, doi: 10.1038/s41467-018-03162-7.

[31] R. W. Stineman, "A Consistently Well-behaved Method of Interpolation," *Creat. Comput.*, vol. 6, pp. 54–57, 1980.

[32] E. Flores-Andrade, L. A. Pascual-Pineda, M. X. Quintanilla-Carvajal, G. F. Gutiérrez-López, C. I. Beristain, and E. Azuara, "Fractal surface analysis and thermodynamic properties of moisture sorption of calcium–sucrose powders," *Dry. Technol.*, vol. 36, no. 9, pp. 1128–1141, 2018, doi: 10.1080/07373937.2017.1387793.

[33] D. F. Othmer, "Correlating Vapor Pressure and Latent Heat Data: A new plot," *Ind. Eng. Chem.*, vol. 32, no. 6, pp. 841–856, 1940, doi: 10.1021/ie50366a022.

[34] H. H. Rowley, and W. B. Innes, "Relationships between the spreading pressure, adsorption, and wetting", *The Journal of Physical Chemistry*, vol. 46, no. 7, pp. 694-705, 1942.

[35] A. Wexler, "Vapor pressure formulation for water in range 0 to 100 C. A revision," *J. Res. Natl. Bur. Stand. Sect. A, Phys. Chem.*, vol. 80, no. 5–6, p. 775, 1976.

[36] L. A. Pascual-Pineda *et al.*, "Micropores and Their Relationship with Carotenoids Stability: A New Tool to Study Preservation of Solid Foods," *Food Bioprocess Technol.*, vol. 7, no. 4, pp. 1160–1170, 2014, doi: 10.1007/s11947-013-1162-0.

[37] L. Acosta-Domínguez, R. Salazar, M. Jiménez, and E. Azuara, "Thermodynamic analysis as a useful tool to study the physical properties of sweet-potato starch films reinforced with alginate microparticles," *Polym. Compos.*, vol. 42, no. 7, pp. 3380–3390, 2021, doi:

10.1002/pc.26065.

[38] F. Garbassi, L. Balducci, P. Chiurlo, and L. Deiana, “A study of surface modification of silica using XPS, DRIFT and NMR,” *Appl. Surf. Sci.*, vol. 84, no. 2, pp. 145–151, 1995, doi: 10.1016/0169-4332(94)00469-2.

[39] X. Wang, W. Zimmermann, K. C. Ng, A. Chakraboty, and J. U. Keller, “Investigation on the isotherm of silica gel+water systems,” *J. Therm. Anal. Calorim.*, vol. 76, pp. 659–669, 2004.

[40] “Nanoshel LLC.” https://www.nanoshel.com/ (accessed Jul. 29, 2021).

[41] T. A. Vu *et al.*, “Isomorphous substitution of Cr by Fe in MIL-101 framework and its application as a novel heterogeneous photo-Fenton catalyst for reactive dye degradation,” *RSC Adv.*, vol. 40, no. 78, pp. 41185–41194, 2014, doi: 10.1039/c4ra06522k.

[42] Y. Li, Z. Tang, and C. Chen, “The modulating effect of ethanol on the morphology of a zr-based metal–organic framework at room temperature in a cosolvent system,” *Crystals*, vol. 11, no. 4, 2021, doi: 10.3390/cryst11040434.

[43] E. F. Vansant, P. Van Der Voort, and K. C. Vrancken, “Chapter 3 The surface chemistry of silica,” in *Studies in Surface Science and Catalysis*, 1995, pp. 59–77.

[44] A. A. Christy and P. K. Egeberg, “Quantitative determination of surface silanol groups in silicagel by deuterium exchange combined with infrared spectroscopy and chemometrics,” *Analyst*, vol. 130, no. 5, pp. 738–744, 2005, doi: 10.1039/b501895c.

[45] Y. Yang, T. Y. Gan, and X. Tan, “Spatiotemporal changes of drought characteristics and their dynamic drivers in Canada,” *Atmos. Res.*, vol. 232, no. August 2019, p. 104695, 2020, doi: 10.1016/j.atmosres.2019.104695.

[46] L. Liu, S. Tan, T. Horikawa, D. D. Do, D. Nicholson, and J. Liu, "Water adsorption on carbon - A review," *Adv. Colloid Interface Sci.*, vol. 250, pp. 64–78, 2017, doi: 10.1016/j.cis.2017.10.002.

[47] A. Chakraborty, B. B. Saha, S. Koyama, K. C. Ng, and K. Srinivasan, "Adsorption thermodynamics of silica gel-water systems," *J. Chem. Eng. Data*, vol. 54, no. 2, pp. 448–452, 2009, doi: 10.1021/je800458k.

[48] K. C. Ng *et al.*, "Experimental investigation of the silica gel-water adsorption isotherm characteristics," *Appl. Therm. Eng.*, vol. 21, no. 16, pp. 1631–1642, 2001, doi: 10.1016/S1359-4311(01)00039-4.

[49] H. T. Chua, K. C. Ng, A. Chakraborty, N. M. Oo, and M. A. Othman, "Adsorption characteristics of silica gel + water systems," *J. Chem. Eng. Data*, vol. 47, no. 5, pp. 1177–1181, 2002, doi: 10.1021/je0255067.

[50] H. Kim *et al.*, "Characterization of Adsorption Enthalpy of Novel Water-Stable Zeolites and Metal-Organic Frameworks," *Sci. Rep.*, vol. 6, no. November 2015, pp. 1–8, 2016, doi: 10.1038/srep19097.

[51] E. T. Jaynes, "Gibbs vs Boltzmann Entropies," *Am. J. Phys.*, vol. 33, no. 5, pp. 391–398, 1965, doi: 10.1119/1.1971557.

[52] D. Wu, X. Guo, H. Sun, and A. Navrotsky, "Interplay of Confinement and Surface Energetics in the Interaction of Water with a Metal-Organic Framework," *J. Phys. Chem. C*, vol. 120, no. 14, pp. 7562–7567, 2016, doi: 10.1021/acs.jpcc.5b12239.

[53] A. Grosman and C. Ortega, "Capillary Condensation in Porous Materials . Hysteresis and Interaction without Pore Blocking / Percolation Process," *Langmuir*, vol. 24, no. 8, pp. 3977–3987, 2008.